INITIAL MODELING OF ELECTRON CLOUD BUILDUP IN THE FINAL-FOCUS QUADRUPOLE MAGNETS OF THE SUPERKEKB POSITRON RING

J. A. Crittenden, CLASSE*, Cornell University, Ithaca, NY 14850, USA

Abstract

We present modeling results for electron cloud buildup in the final-focus quadrupole magnet nearest the interaction point in the SuperKEKB positron storage ring. The calculations employ as input recently obtained estimates of synchrotron radiation absorption rates on the vacuum chamber wall including the effect of photon scattering. While the effect both adds to and subtracts from photoelectron production at the points in the ring where unscattered photons strike the wall, it also produces cloud in the other regions. Results for beam-pipe-averaged and beam-averaged cloud densities are presented, as are estimates for the contribution to the fractional vertical coherent tune shift. The effect of the strong magnetic fields is studied and the dependence on the vacuum chamber surface secondary yield characteristics is considered. Cloud buildup is modeled with a 2D particle-in-cell macroparticle tracking code validated using recent measurements of electron trapping in a quadrupole magnet at the Cornell Electron Storage Ring Test Accelerator.

INTRODUCTION

The SuperKEKB e+e- collider is scheduled to begin operation in 2016. It will provide measurements of the decays of bound states of B quarks with unprecedented statistical precision. High luminosity operation depends on the strong field gradient region provided by the superconducting final-focus quadrupole magnets within 2 m of the interaction point (IP), with beta function values reaching as high 3000 m. Tune shifts near the interaction region have been calculated to be the dominant contribution to the total tune shift around the ring [1, 2]. These calculations did not include contributions from the final-focus quadrupole magnets. Recently, calculations of the synchrotron radiation distribution around the 4 GeV SuperKEKB positron ring including the effects of photon scattering on the walls of the vacuum chamber have become available [3]. The results show substantial rates of absorption in the final-focus quadrupoles, comparable to the highest rates in the arcs of the ring. In addition, the first measurements of electron trapping in a high-energy positron storage ring have been obtained recently in the context of the Cornell Electron Storage Ring Test Accelerator (CᴇꜱʀTA) program [4], allowing validation of an electron cloud buildup model for an ambient quadrupole magnetic field. The model successfully reproduced the trapping fraction when parameters were tuned to the signals observed in a time-resolving electron detec-

tor. Here we report on the initial application of this model for the case of cloud buildup in the upstream final-focus quadrupole nearest the IP in the SuperKEKB positron storage ring.

SUPERKEKB FINAL-FOCUS QUADRUPOLE MAGNETS

The final-focus quadrupole magnet nearest the IP in the positron ring, designated QC1RP, is 334 mm long and its center is located 935 mm from the IP. It operates at a field gradient of 68.74 T/m [5]. Superposed on this high-gradient quadrupole field is a non-uniform longitudinal field from the BELLE-II solenoid compensation magnets, as shown in Fig. 1 [6]. The longitudinal component of this field varies from about 1 T to approximately 2.5 T over the 334-mm length of the QC1RP magnet. For the purpose of the model described here, the solenoid compensation field has been assumed to be 2 T, rotated around the vertical axis by half the crossing angle, i.e. $\frac{83}{2}$ mrad, relative to the axis of the quadrupole field. Copper and TiN-coated surfaces are under consideration for the cylindrical, 21-mm-inner-diameter vacuum chamber.

PHOTON TRACKING AND CLOUD BUILDUP MODELING

The results from the X-ray photon scattering and tracking code which are used as input to the electron cloud buildup modeling in the QC1RP magnet [3] are shown in Fig. 2. Together with the overall photon absorption rate, the azimuthal distribution of absorbed photons (Fig. 2a)) is an important consideration for cloud development in a magnetic field, since cloud electrons are guided by the field lines, emphasizing the contribution of those produced on field lines near the beam which intersect the vacuum chamber wall. Figure 2b) shows the photon absorption rate to
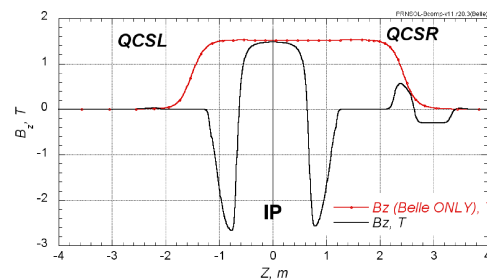

Figure 1: Longitudinal magnetic field component from the BELLE-II solenoid alone (red) and including the compensation field (black).

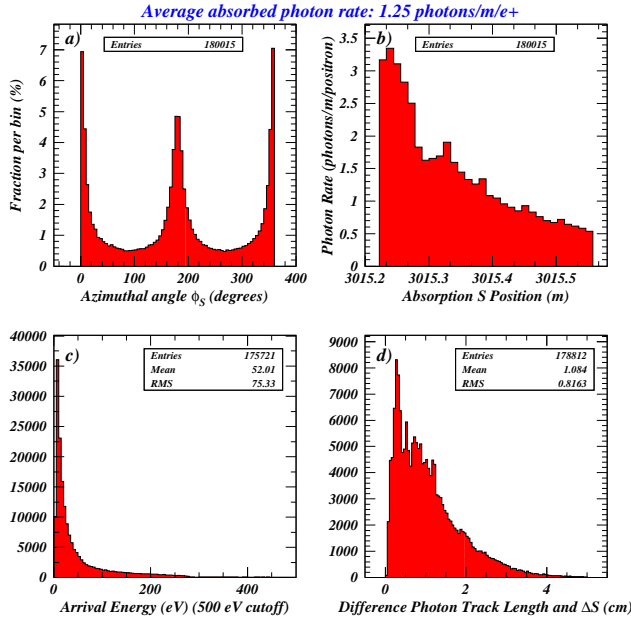**Average absorbed photon rate: 1.25 photons/m/e+**

Figure 2: Distributions of photons absorbed in the final-focus quadrupole magnet QC1RP including the effects of photon scattering in the positron ring. a) Distribution in azimuthal angle ϕ_s of the absorbed photon position around the 21-mm-diameter beam pipe. b) Distribution of absorbed photon locations in the arc coordinate S of the positron orbit. c) Distribution of absorbed photon energies below 500 eV. d) Difference of photon and positron orbit track lengths.

vary by about a factor of 6 over the length of the magnet. For this initial study, we have used the average rate of 1.25 photons/m/positron. The absorbed photon energy distribution shown in Fig. 2c) informs the choice of photoelectron production energy distribution. For the present model, a distribution peaking at 10 eV with a small power-law tail yielding energies above 100 eV at the percent level was used. Finally, Fig. 2d) shows that most of the absorbed photons have scattered sufficiently to de-synchronize their arrival time with the 6-mm-long positron bunch passage. The cloud buildup is calculated in the approximation that the photoelectrons are not accelerated by the positron bunch when produced.

The cloud buildup modeling employs the code ECLOUD [7, 8], which includes models for photoelectron generation kinematics, for time-sliced macroparticle tracking in the 2D electrostatic fields sourced by the beam and the cloud, and 3D tracking in magnetic fields, and a detailed model of the secondary emission process at the vacuum chamber wall. It has been used to model a variety of cloud buildup measurements using time-resolving electron detectors [9], including the case of an ambient magnetic quadrupole field [4], as well as CESRTA coherent tune shift measurements [10]. The photoelectron generation algorithm allows great flexibility in choosing photoelectron energy distributions and quantum efficiencies as a function of production position, but is rather ad hoc. Here we have assumed a quantum efficiency of 10% independent of position, similar to the value used for the coherent tune shift modeling in the CESR aluminum vacuum chamber. The

secondary emission yield (SEY) model is parameterized in the manner described by Furman and Pivi [11] for the case of copper. We consider three cases: as-received copper, beam-conditioned copper, and TiN coating. Table 1 shows the parameters chosen according to CESRTA in-situ SEY measurements of the beam conditioning of copper surfaces [12], complemented by results from the CESRTA witness bunch measurements isolating the determination of the elastic yield value [9]. In general, the modeling

Table 1: Secondary yield model parameters used for three vacuum chamber surfaces.

Parameter	Copper as-received	Copper conditioned	TiN
δ_{true}	1.9	1.0	1.0
$E_{\text{peak}}^{\text{true}}$ (eV)	276	330	420
δ_{elastic}	0.5	0.5	0.1
$\delta_{\text{rediffused}}$	0.2	0.2	0.

results indicate the cloud to be dominated by the secondary yield process for the copper surfaces, with a dependence on the assumed quantum efficiency much weaker than linear, while the dependence on quantum efficiency is nearly linear for the case of TiN coating.

MODELED CLOUD DENSITY AND TUNE SHIFT

The electron cloud buildup simulation has been performed for the case of 4 GeV 6-mm-long (RMS) bunches carrying 9.4×10^{10} positrons each, spaced by 4 ns. The transverse dimensions of the beam are modeled as Gaussian with RMS values of 0.40 mm horizontally and 0.33 mm vertically. These are approximations of the beam cross section, which varies along the length of the Q1CRP magnet from 0.35 mm to 0.20 mm horizontally and from 0.38 mm to 0.33 mm vertically. Figure 3 shows the beam-pipe-averaged cloud density buildup with combined quadrupole and off-axis solenoidal magnetic fields. The saturation values are reached after the passage of about 50 bunches at the level of 2.8×10^{14} m^{-3}, 1.5×10^{14} m^{-3}, and 7.0×10^{13} m^{-3} for SEY parameters of as-received copper, beam-conditioned copper and TiN-coating, respectively. The cloud density averaged
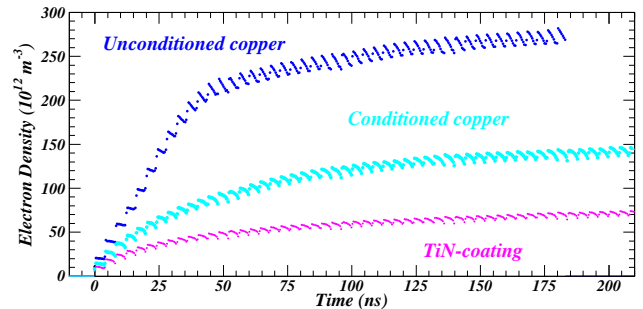

Figure 3: Beam-pipe-averaged electron cloud buildup assuming secondary yield values typical of as-received copper, beam-conditioned copper and TiN-coating.
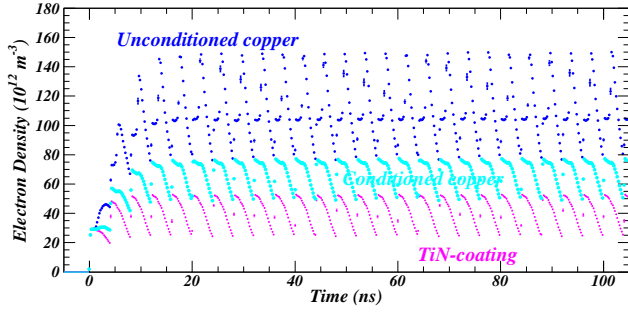
Figure 4: Beam-pipe-averaged cloud densities in the absence of the quadrupole and solenoidal magnetic fields.

over the beam transverse cross section, evaluated just prior to the arrival of the bunch (not shown), stabilizes at values of about 6.5×10^{13} m^{-3}, 3.5×10^{13} m^{-3}, and 1.6×10^{13} m^{-3} after 15 bunch passages for the three cases. While such cloud densities are three orders of magnitude larger than the ring-average density estimated in Ref. [1], the 334-mm length of QC1RP results in a contribution of only a few percent to the fast head-tail instability threshold value of 2.2×10^{11} m^{-3} [2]. The contribution from the QC1RP magnet with a copper surface before beam conditioning raises the ring-averaged cloud density from 2.4×10^{10} m^{-3} to 3.1×10^{10} m^{-3}.

Figure 4 shows the beam-pipe-averaged density associated with cloud buildup in the absence of magnetic field, as may be the case during a commissioning phase of operations. The magnetic field evidently prevents most of the cloud decay during the 4-ns interval between bunches. The corresponding beam-averaged cloud densities for the three surfaces are similar, reaching values near $1 - 2 \times 10^{13}$ m^{-3}.

The contribution to the fractional coherent tune shift can be calculated from the electric field gradient produced by the cloud charge at the beam via the relation

$$\Delta \nu_{\mathrm{X/Y}} = \frac{\beta_{\mathrm{X/Y}} \, \Delta L}{4\pi E_{\mathrm{beam}}/\mathrm{eV}} \, \frac{\mathrm{d}E_{\mathrm{X/Y}}}{\mathrm{d}X/Y}, \qquad (1)$$

where ΔL is the length of the region contributing to the tune shift. As shown in Fig. 5, the vertical beta function reaches values greater than 3000 m in the QC1RP magnet. Assuming this value $\beta_{\mathrm{Y}} = 3000$ m, the fractional vertical tune shift is given by $\Delta \nu_{\mathrm{Y}} = 2.0 \times 10^{-8} \frac{\mathrm{d}E_{\mathrm{Y}}}{\mathrm{d}Y}$ when the field gradient is expressed in units of V/m^2. The cloud space charge field is calculated in 15 time slices during passage of each bunch. The average value of vertical field gradient on the beam axis is shown as a function of buildup time in Fig. 6. For the case of an as-received copper surface, the field gradient of 800 kV/m^2 results in a contribution to the tune shift
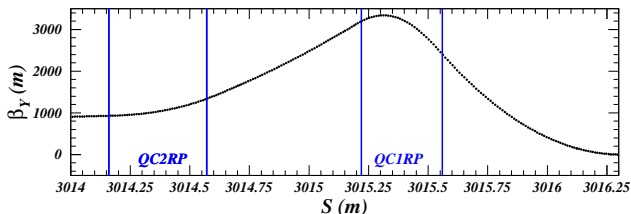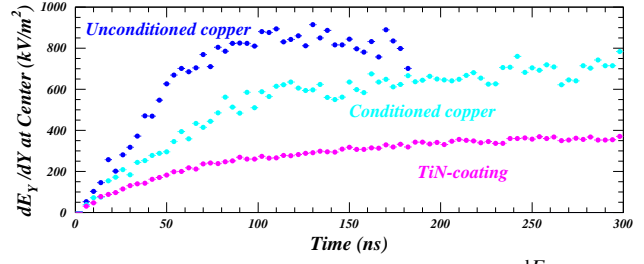

Figure 5: Vertical beta function β_{Y} in the final-focus region

Figure 6: Electron cloud vertical field gradient $\frac{\mathrm{d}E_{\mathrm{Y}}}{\mathrm{d}Y}$ on the beam axis versus cloud buildup time.

by the QC1RP magnet alone of about 0.016, which is about a factor of 15 larger than the tune shift in the rest of the ring, which itself is dominated by the near-IR region [2]. The TiN coating reduces this contribution by about a factor of two.

SUMMARY AND OUTLOOK

The first estimates of electron cloud buildup in the superconducting final-focus quadrupole magnet nearest the SuperKEKB IP in the 4-GeV positron ring indicate cloud densities 2-3 orders of magnitude higher than previous estimates, reaching 2.5×10^{14} m^{-3}. Beam conditioning of the as-received interior copper surface of the vacuum chamber can be expected to reduce the beam-pipe-averaged density by a factor of 2. The density resulting from a TiN coating is lower by an additional factor of 2. Most of the cloud is not near the beam, so the modeled cloud densities averaged over the transverse beam cross section at bunch arrival time are a factor of 4 lower than the beam pipe averages. Since this density is limited to a length of 0.334 m, it increases present estimates of the ring-averaged density by about 30% in the worst case. If the combined high-gradient quadrupole and off-axis solenoidal magnetic fields are absent, the cloud decays substantially during the 4-ns interval between bunch passages and the beam-averaged densities are about $1 - 2 \times 10^{13}$ m^{-3}.

The contribution of this cloud to the fractional vertical coherent tune shift based on space charge calculations of the electric field gradient on the beam axis is projected to be a factor of 15 larger than previous estimates of the contribution from the rest of the ring, owing to the large beta function value of about 3000 m and the large field gradient values of 400-800 kV/m^2.

Several underlying assumptions in these initial modeling results require further study. The effect on cloud buildup of the variation of the solenoidal field along the length of the QC1RP magnet must be estimated. Non-linear effects can also be expected when the factor of 6 longitudinal variation of the absorbed photon rate is taken into account. Also, systematic uncertainties resulting from the ad hoc treatment of the quantum efficiency for photoelectron production, the assumed production kinetic energy distribution, and the fraction which experiences a kick from the positron bunch, must be calculated. In addition, calculations of electron buildup in the other final-focus quadrupole magnets are needed, including those in the electron ring.

REFERENCES

[1] Y. Suetsugu *et al.*, "Design and Construction of the SuperKEKB Vacuum System," *J. Vac. Sci. Technol. A* **30**, 031602 (May 2012).

[2] K. Ohmi & D. Zhou, "Study of Electron Cloud Effects in SuperKEKB," in *IPAC2014: Proceedings of the 5th International Particle Accelerator Conference, Dresden, Germany*, C. Petit-Jean-Genaz *et al.*, Eds., JACoW, Geneva, Switzerland (2014), p. 1597–1599.

[3] J. A. Crittenden *et al.*, "Synchrotron Radiation Analysis of the SuperKEKB Positron Storage Ring," in *IPAC2015: Proceedings of the 6th International Particle Accelerator Conference, Richmond, Virginia, USA*, C. Petit-Jean-Genaz *et al.*, Eds., JACoW, Geneva, Switzerland (2015).

[4] M. Billing *et al.*, "Measurement of electron trapping in the Cornell Electron Storage Ring," *Phys. Rev. ST Accel. Beams* **18**, p. 041001 (apr 2015).

[5] N. Ohuchi *et al.*, "Design of the Superconducting Magnet System for the SuperKEKB Interaction Region," in *PAC 2013: Proceedings of the 2013 Particle Accelerator Conference, Pasadena, CA, USA*, T. Satogata, C. Petit-Jean-Genaz & V. Schaa, Eds., JACoW (2013), p. 843–845.

[6] H. Yamaoka *et al.*, "Solenoid Field Calculation of the SuperKEKB Interaction Region," in *Proceedings of the 2012 International Particle Accelerator Conference, New Orleans, LA*, IEEE (2012), p. 3548–3550.

[7] G. Rumolo & F. Zimmermann, "Practical User Guide for ECloud," Tech. Rep. CERN-SL-Note-2002-016-AP, CERN, Geneva, Switzerland (May 2002).

[8] G. Rumolo, F. Ruggiero & F. Zimmermann, "Simulation of the Electron-Cloud Build Up and Its Consequences on Heat Load, Beam Stability, and Diagnostics," *Phys. Rev. ST Accel. Beams* **4**, 012801 (Erratum: 029901) (Jan. 2001).

[9] J. A. Crittenden & J. P. Sikora, "Electron Cloud Buildup Characterization Using Shielded-Pickup Measurements and Custom Modeling Code at CᴇꜱʀTA," in *Proceedings of ECLOUD 2012: Joint INFN-CERN-EuCARD-AccNet Workshop on Electron-Cloud Effects, La Biodola, Elba, Italy*, R. Cimino, G. Rumolo & F. Zimmermann, Eds., CERN, Geneva, Switzerland (2013), CERN-2013-002, p. 241–250.

[10] J. A. Crittenden *et al.*, "Progress in Studies of Electron-cloud-induced Optics Distortions at CesrTA," in *Proceedings of the 2010 International Particle Accelerator Conference, Kyoto, Japan*, ACFA (2010), p. 1976–1978.

[11] M. A. Furman & M. T. F. Pivi, "Probabilistic Model for the Simulation of Secondary Electron Emission," *Phys. Rev. ST Accel. Beams* **5**, 124404 (Dec. 2002).

[12] W. Hartung *et al.*, "Measurements of Secondary Electron Yield of Metal Surfaces and Films with Exposure to a Realistic Accelerator Environment," in *IPAC2013: Proceedings of the 4th International Particle Accelerator Conference, Shanghai, China*, Z. Dai *et al.*, Eds., JACoW (2013), p. 3493–3495.